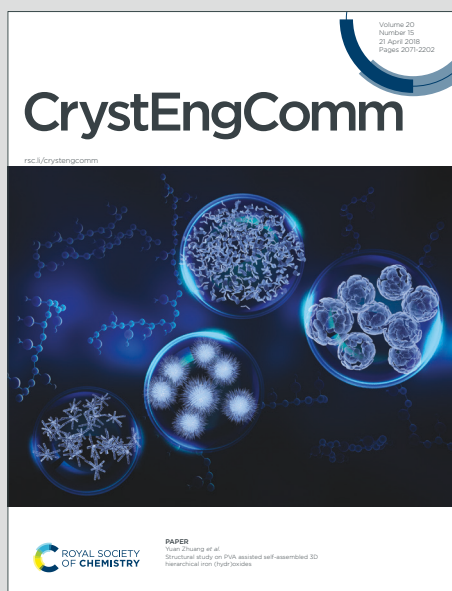


CrystEngComm

Accepted Manuscript

This article can be cited before page numbers have been issued, to do this please use: T. K. Ghosh, P. Mahapatra, S. Jana and A. Ghosh, *CrystEngComm*, 2019, DOI: 10.1039/C9CE00574A.



This is an Accepted Manuscript, which has been through the Royal Society of Chemistry peer review process and has been accepted for publication.

Accepted Manuscripts are published online shortly after acceptance, before technical editing, formatting and proof reading. Using this free service, authors can make their results available to the community, in citable form, before we publish the edited article. We will replace this Accepted Manuscript with the edited and formatted Advance Article as soon as it is available.

You can find more information about Accepted Manuscripts in the [Information for Authors](#).

Please note that technical editing may introduce minor changes to the text and/or graphics, which may alter content. The journal's standard [Terms & Conditions](#) and the [Ethical guidelines](#) still apply. In no event shall the Royal Society of Chemistry be held responsible for any errors or omissions in this Accepted Manuscript or any consequences arising from the use of any information it contains.

Variation of nuclearity from mono-to-tetra-to-hexanuclear Ni^{II} complexes of a Schiff base ligand: Crystal structures and magnetic studies

Tanmoy Kumar Ghosh, Prithwish Mahapatra, Subrata Jana, Ashutosh Ghosh*

Department of Chemistry, University College of Science, University of Calcutta, 92, A.P.C. Road, Kolkata 700 009, India, E-mail address: ghosh_59@yahoo.com

Abstract

Four new Ni^{II} complexes, [Ni(L¹)](NO₃)·1.5H₂O (**1**), [Ni(L¹)][(Ni(HL²)](NO₃)₂·H₂O (**2**), [Ni₄(L²)₂(μ₃-OCH₃)₂(NO₃)](NO₃)·CH₃OH (**3**), [(Ni₆(L²)₂(*o*-van)₂(μ₃-OH)₄](NO₃)₂·H₂O (**4**) where HL¹ = 2- $\{2-(2\text{-aminoethylamino})\text{ethylimino}\}$ methyl}-6-methoxyphenol and H₂L² = *N,N'*-bis(3-methoxysalicylidene)diethylenetriamine), have been synthesized by changing the reaction conditions and stoichiometry of the reactants. Single crystal X-ray diffraction study reveals that complexes **1** and **2** are mononuclear with square planar geometry around Ni^{II} centre whereas complexes **3** and **4** possess tetranuclear and hexanuclear structures, respectively with octahedral Ni^{II} centres. The differences in nuclearity, coordination numbers and geometry of Ni^{II} centres in the complexes have been explained considering flexible coordination modes and denticity of the Schiff base ligands. The variable temperature molar magnetic susceptibility measurements show that tetranuclear Ni^{II}₄ complex (**3**) is ferromagnetically coupled with two exchange couplings $J_1 = 0.64 \text{ cm}^{-1}$ and $J_2 = 8.41 \text{ cm}^{-1}$, whereas hexanuclear Ni^{II}₆ complex (**4**) is antiferromagnetically coupled with four exchange couplings $J_1 = -5.60 \text{ cm}^{-1}$, $J_2 = -9.39 \text{ cm}^{-1}$, $J_3 = -5.18 \text{ cm}^{-1}$ and $J_4 = 3.72 \text{ cm}^{-1}$. The sign and magnitude of these exchange couplings in complexes **3** and **4** are correlated with similar types of reported cubane or defective cubane like Ni^{II} complexes. Electrochemical measurements of these complexes reveal that the Ni^{II} centres are irreversibly reduce with one reduction potential for **1**, **3** and **4**, whereas for **2** the Ni^{II} centres are irreversibly reduce with two reduction potentials.

Introduction

The interest for designed synthesis of discrete multinuclear metal clusters of transition metal ions is primarily due to their aesthetic structural diversity, relevance to significant biological processes in metalloenzymes¹ and fascinating magnetic properties.² The most challenging aspect for the synthesis of such complexes is to control the nuclearity because it depends not only upon the characteristics of metal ions and ligands but also on the metal ion to ligand ratios, counter anions, reaction conditions, solvents used for synthesis etc.³ Discrete polynuclear complexes of most of the 1st transition metal ions are well known. Several of these species are of immense importance for mimicking biologically important reactions⁴ and for understanding the fundamentals for magnetic coupling as well as single molecule magnet behaviour.⁵ Among the ligands of different donor atoms, oxygen donor atoms seem to be the most suitable for their flexible μ_2 - or μ_3 -bridging ability.⁶ For example, the Schiff base ligand, *N,N'*-bis(3-methoxysalicylidene)diethylenetriamine (H_2L^2) contains seven potential donor atoms; three N and four O atoms. Among these four oxygen atoms, two are phenolic and can coordinate to metal ions in monodentate mode or bridging μ_2 - or μ_3 -mode whereas two methoxy oxygen atoms remain either non-coordinated or coordinated rather weakly in monodentate mode. Exploiting this different coordination behaviours of oxygen atoms, quite a few homo- and hetero-metallic transition metal and lanthanide complexes of various nuclearity have been synthesised.⁷ Recently, during working on the synthesis of Zn^{II} complexes of this ligand, we serendipitously obtained di-, tetra- and hexa-nuclear complexes on changing the reaction conditions and ligand to metal ratios.⁸ We are curious to investigate if tailored synthesis of such complexes with desired nuclearity is also possible for other metal ions under similar reaction conditions.

Among the complexes of 1st transition metal ions, those of Ni^{II} deserve special mention for their structural diversity and tendency to form high nuclearity metal clusters, especially with N,O donor ligands. The dinuclear Ni^{II} complexes are the most common but the complexes of higher nuclearity *i.e.* Ni_3 , Ni_4 , Ni_5 , Ni_6 , Ni_7 , Ni_{11} , Ni_{18} , Ni_{20} , Ni_{21} , Ni_{32} etc. are also well known.⁹ In addition to the structural diversity, magnetic properties of the high nuclearity Ni^{II} complexes attract the potential interest of researchers. A variety of Ni^{II} complexes with different geometries like; cubane, defective cubane, double cubane etc. are reported in literature and their fascinating magnetic behaviours are investigated by various groups.^{5a,5b,5d,5f} It has been found that the magnetic interactions may change from antiferro-

to ferromagnetic with the small changes in structural geometry, bridging mode and angle of coordinating atoms of ligands.^{9c,9d,9f} The nuclearity and nature of magnetic interactions are found to be extremely important for the intriguing single molecule magnet properties exhibited by several multinuclear Ni^{II} complexes. Therefore, our focus is to synthesize Ni^{II} complexes with diverse but desired nuclearities and investigate the magnetic behaviours.

In the present work, we report synthesis and structural characterization of four complexes, [Ni(L¹)](NO₃)·1.5H₂O (**1**), [Ni(L¹)]Ni(HL²)(NO₃)₂·H₂O (**2**), [Ni₄(L²)₂(μ₃-OCH₃)₂(NO₃)](NO₃)·CH₃OH (**3**) and [(Ni₆(L²)₂(*o*-van)₂(μ₃-OH)₄](NO₃)₂·H₂O (**4**) where HL¹ = 2-[2-(2-aminoethylamino)ethylimino]methyl}-6-methoxyphenol and H₂L² = *N,N'*-bis(3-methoxysalicylidene)diethylenetriamine). Complexes **2–4** have been synthesized by reacting H₂L² with Ni(II) nitrate on varying the metal:ligand ratios and reaction conditions. The presence of the Ni^{II} complex of monocondensed ligand HL¹ as a component of cocrystalline complex **2**, encourages us to synthesize the complex **1** which is solely of the monocondensed ligand. The electrochemical properties of all four complexes have been studied by cyclic voltammetry measurements. The temperature dependent molar magnetic susceptibility and isothermal magnetization measurements are performed for complexes **3** and **4** in which Ni^{II} centres are paramagnetic. A magneto structural correlation has also been drawn considering similar types of reported multinuclear Ni^{II} complexes.

Experimental Section

Starting materials

All chemicals and solvents were of reagent grade and were commercially available. They were used without any further purification.

Synthesis of Schiff base ligand [*N,N'*-bis(3-methoxysalicylidene)diethylenetriamine] (H₂L²)

The Schiff base ligand H₂L² were prepared by following standard literature method:⁸ 10 mmol (1.521 g) of *o*-vanillin was mixed with 5 mmol (0.540 mL) of diethylenetriamine in methanol (20 mL). The resulting yellow methanolic solution was refluxed for 2 h. The volume of the resulting solution was reduced to 5 mL on keeping upon a water bath. The solution was cooled and then 10 mL diethyl ether was added to it. The resulting mixture was

kept at $-5\text{ }^{\circ}\text{C}$ in a refrigerator for 2 days, when the desired Schiff base (H_2L^2) separated out as yellow solid.

Synthesis of the complex $[\text{Ni}(\text{L}^1)](\text{NO}_3)\cdot 1.5\text{H}_2\text{O}$ (1)

Complex **1** was prepared by the reaction of two precursors, bis(*o*-vanillin)nickel(II) dihydrate and bis(diethylenetriamine)nickel(II). Bis(*o*-vanillin)nickel(II)dihydrate was prepared according to standard literature method;¹⁰ 10 mmol (1.521 g) of *o*-vanillin was mixed with 5 mmol (1.45 g) of $\text{Ni}(\text{NO}_3)_2\cdot 6\text{H}_2\text{O}$ in methanol (30 mL) with constant stirring. Then triethylamine 10 mmol (1.4 mL) was added drop wise to the above mixture and stirring was continued for 30 min. A green precipitate separated out and was collected by filtration. The precipitate was washed with methanol. The other precursor bis(diethylenetriamine)nickel(II) was prepared¹¹ by mixing 10 mmol (1.08 mL) of diethylenetriamine with 5 mmol (1.45 g) of $\text{Ni}(\text{NO}_3)_2\cdot 6\text{H}_2\text{O}$ in methanol (30 mL). The mixture was stirred for 30 min when a violet solid separated out, which was collected by filtration. Then, bis(diethylenetriamine)nickel(II) (1.94 g, 5 mmol) was dissolved in 20 mL methanol and a methanolic solution (20 mL) bis(*o*-vanillin)nickel(II) dihydrate (1.81 g, 5 mmol) was added to it and put under reflux for 5 h. The colour of the solution was turned into deep red. The solution was filtered and left in open atmosphere. The deep red X-ray quality single crystals were obtained after a few days on slow evaporation of the solvent. The crystals were filtered out from the solution and air dried.

Complex 1: Yield 1.241g (65%) $\text{C}_{24}\text{H}_{38}\text{N}_8\text{Ni}_2\text{O}_{13}$ (764.00). Calculated C, 37.73; H, 5.01; N, 14.67; Found C, 37.62; H, 5.10; N, 14.79; IR: $\nu_{(\text{N-H})} = 3170, 3185\text{ cm}^{-1}$, $\nu_{(\text{C=N})} = 1618\text{ cm}^{-1}$, $\nu_{(\text{NO}_3)} = 1384\text{ cm}^{-1}$.

Synthesis of complex $[\text{Ni}(\text{L}^1)][(\text{Ni}(\text{HL}^2))(\text{NO}_3)_2\cdot \text{H}_2\text{O}]$ (2)

A methanolic solution (20 mL) of $\text{Ni}(\text{NO}_3)_2\cdot 6\text{H}_2\text{O}$ (1 mmol, 0.290 g) was added to the methanolic solution (20 mL) of H_2L^2 (1 mmol, 0.371 g) with constant stirring. The resulting solution was stirred for further 2 h. Diffraction quality red single crystals were obtained after a few days on slow diffusion of diethyl ether into the solution.

Complex 2: Yield 0.325 g (65%) $\text{C}_{32}\text{H}_{44}\text{N}_8\text{Ni}_2\text{O}_{13}$ (866.13). Calculated C, 44.37; H, 5.12; N, 12.94; Found C, 44.21; H, 5.20; N, 12.89; IR: $\nu_{(\text{N-H})} = 3190\text{ cm}^{-1}$, $\nu_{(\text{C=N})} = 1625\text{ cm}^{-1}$, $\nu_{(\text{NO}_3)} = 1384\text{ cm}^{-1}$.

Synthesis of the complex $[\text{Ni}_4(\text{L}^2)_2(\mu_3\text{-OCH}_3)_2(\text{NO}_3)](\text{NO}_3)\cdot\text{CH}_3\text{OH}$ (**3**)

A methanolic solution (20 mL) of $\text{Ni}(\text{NO}_3)_2\cdot 6\text{H}_2\text{O}$ (2 mmol, 0.580 g) was mixed with methanolic solution (20 mL) of H_2L^2 (1 mmol, 0.371 g) with constant stirring. Then the triethylamine (2 mmol, 0.28 mL) was added drop wise to the mixture. The resulting solution was stirred for another 2 h. Green single crystals for X-ray diffraction were obtained by slow diffusion of diethyl ether into the mother liquor.

Complex 3: Yield 0.379 g (62%) $\text{C}_{43}\text{H}_{52}\text{N}_8\text{Ni}_4\text{O}_{17}$ (1187.69). Calculated C, 43.48; H, 4.41; N, 9.43; Found C, 43.38; H, 4.59; N, 9.48; IR: $\nu_{(\text{N-H})} = 3200\text{ cm}^{-1}$, $\nu_{(\text{C=N})} = 1615\text{ cm}^{-1}$, $\nu_{(\text{NO}_3)} = 1384\text{ cm}^{-1}$.

Synthesis of the complex $[(\text{Ni}_6(\text{L}^2)_2(o\text{-van}))_2(\mu_3\text{-OH})_4](\text{NO}_3)_2\cdot\text{H}_2\text{O}$ (**4**)

A methanolic solution (25 mL) of $\text{Ni}(\text{NO}_3)_2\cdot 6\text{H}_2\text{O}$ (3 mmol, 0.870 g) was added to the methanolic solution (15 mL) of H_2L^2 (1 mmol, 0.371 g). To this solution triethylamine (2 mmol, 0.28 mL) and *o*-vanillin (1 mmol, 0.152 g) were added. The resulting solution was refluxed for 3 h, cooled and filtered. The X-ray diffraction quality green single crystals were obtained on slow diffusion of diethyl ether into the filtrate.

Complex 4: Yield 0.480 g (60%) $\text{C}_{56}\text{H}_{64}\text{N}_8\text{Ni}_6\text{O}_{25}$ (1601.41). Calculated C, 42.00; H, 4.03; N, 7.00; Found C, 42.09; H, 3.94; N, 6.95; IR: $\nu_{(\text{O-H})} = 3400\text{ cm}^{-1}$, $\nu_{(\text{N-H})} = 3210\text{ cm}^{-1}$, $\nu_{(\text{C=N})} = 1638\text{ cm}^{-1}$, $\nu_{(\text{NO}_3)} = 1384\text{ cm}^{-1}$.

Physical measurements

Elemental analyses (C, H and N) were performed using a Perkin-Elmer 2400 series II CHN analyzer. IR spectra in KBr pellets ($4000\text{--}500\text{ cm}^{-1}$) were recorded using a Perkin-Elmer RXI FTIR spectrophotometer. Temperature-dependent magnetic measurements of powdered samples of **3** and **4** were performed by a superconducting quantum interference device vibrating sample magnetometer (SQUID-VSM) with an applied field of 500 Oe in the temperature range 2–300 K. Pascal's constants were used to quantify diamagnetic corrections to the molar paramagnetic susceptibility and a correction was applied for the sample holder. Field dependent magnetic measurements (0–5 Tesla) were carried out at 2 K for **3** and at 2.5 K for **4**.

Electrochemical measurements

The electrochemical studies of all four complexes **1–4** were performed using a Basi-Epsilon C3 Cell instrument at a scan rate of 100 mVs⁻¹ within the potential range of 0 to -1.80 V vs. Ag/AgCl. Cyclic voltammograms were carried out using 0.1 M TBAP as supporting electrolyte and 1.0×10⁻³ M of complexes in acetonitrile solution which are deoxygenated by argon purging. The working electrode was a glassy carbon disk (0.32 cm²) which was polished with alumina solution, washed with absolute acetone and acetonitrile, and air dried before each electrochemical run. The reference electrode was Ag/AgCl, with platinum as counter electrode. All experiments were performed in standard electrochemical cells at 25 °C.

X-ray Crystallographic data collection and refinement

Suitable single crystals of complexes **1–4** were mounted on a Bruker-AXS SMART APEX II diffractometer equipped with a graphite monochromator and Mo-K α ($\lambda = 0.71073$ Å) radiation. The structure was solved by direct methods and refined by full-matrix least squares on F² using the SHELXL-2014 package¹² and Olex2 program.¹³ Non-hydrogen atoms were refined with anisotropic thermal parameters. The hydrogen atoms bonded to carbon were included in geometric positions and given thermal parameters equivalent to 1.2 times those of the atom to which they were attached. All other hydrogen atoms were placed in their geometrically idealized positions and constrained to ride on their parent atoms except for the hydrogen atoms of the interstitial two water molecules in complex **1** and one water molecule in complex **4**, and a methanol solvent molecule in complex **3** that could not be located in the Fourier map. The interstitial one water molecule for complexes **1** and **4**, and one nitrate ion in complex **1** were refined isotropically. The methanol molecule in complex **3** was disordered and a model was refined in which two different sites were located for the carbon and oxygen atoms. Successful convergence was indicated by the maximum shift/error of 0.001 for the last cycle of the least squares refinement. Absorption corrections were carried out using the SADABS program.¹⁴ Data collection, structure refinement parameters, and crystallographic data for complexes **1–4** are given in Table 1.

Table 1: Crystal data and structure refinement of complexes 1–4.

Complex	1	2	3	4
Chemical formula	C ₂₄ H ₃₈ N ₈ Ni ₂ O ₁₃	C ₃₂ H ₄₄ N ₈ Ni ₂ O ₁₃	C ₄₃ H ₅₂ N ₈ Ni ₄ O ₁₇	C ₅₆ H ₆₄ N ₈ Ni ₆ O ₂₅
Formula weight	764.00	866.13	1187.69	1601.29
Crystal system	Monoclinic	Monoclinic	Monoclinic	Monoclinic
Space group	<i>P</i> 2 ₁ / <i>n</i>	<i>P</i> 2 ₁ / <i>c</i>	<i>P</i> 2 ₁ / <i>c</i>	<i>C</i> ₂ / <i>c</i>
<i>a</i> (Å)	5.1874(4)	22.233(4)	13.838(4)	20.212(11)
<i>b</i> (Å)	34.715(3)	7.3217(14)	29.260(9)	22.656(11)
<i>c</i> (Å)	18.1886(15)	23.045(4)	14.867(4)	16.048(8)
β (°)	90.275(2)	101.296(4)	116.548(4)	121.342(10)
<i>V</i> (Å) ³	3275.4(5)	3678.7(12)	5385(3)	6276(6)
<i>Z</i>	4	4	4	4
ρ_{calc} (g cm ⁻³)	1.549	1.564	1.465	1.695
<i>T</i> (K)	292	299	296	296
μ (Mo <i>K</i> α) (mm ⁻¹)	1.224	1.100	1.450	1.853
<i>F</i> (000)	1592.0	1808.0	2456.0	3296.0
<i>R</i> (int)	0.081	0.049	0.072	0.102
Total reflections	104175	86877	37759	13643
Unique reflections	8159	6675	9473	4749
Reflections with <i>I</i> > 2 σ (<i>I</i>)	5916	5907	6223	2408
[<i>I</i> > 2 σ (<i>I</i>)] <i>R</i> ₁ ^a , <i>wR</i> ₂ ^b	0.0806, 0.2110	0.038, 0.099	0.0924, 0.2922	0.0617, 0.2121
<i>R</i> (all data)	0.1166	0.0448	0.1299	0.1349
GOF ^c	1.145	1.115	1.087	1.008
Residual electron density, e/Å ⁻³	-0.54, 1.27	-0.45, 0.52	-0.89, 0.1.26	-0.60, 1.12

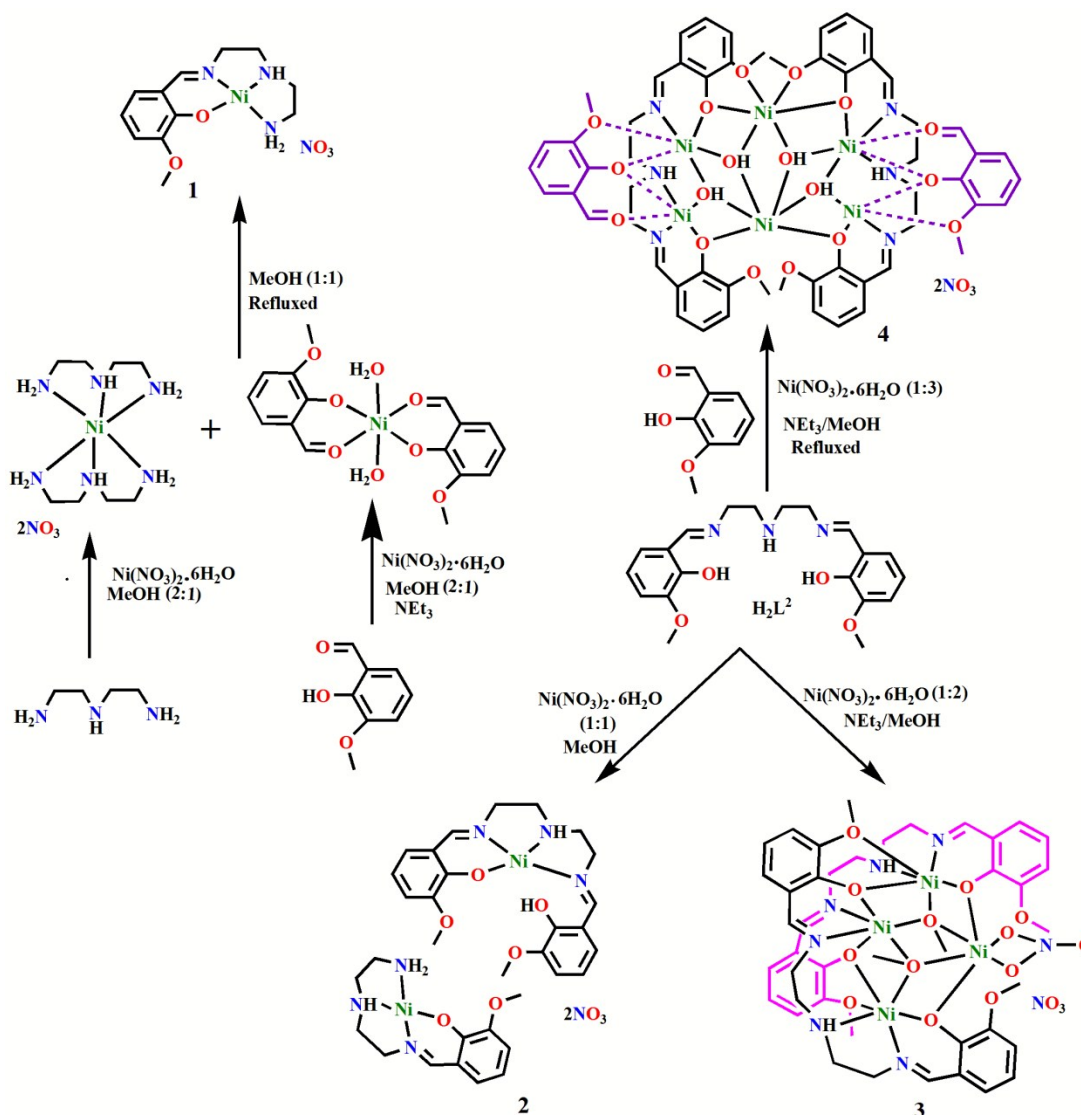
$$^a R_1 = \sum ||F_o| - |F_c|| / \sum |F_o|, ^b wR_2 (F_o^2) = [\sum [w(F_o^2 - F_c^2)^2 / \sum w F_o^4]^{1/2} \text{ and } ^c \text{GOF} = [\sum [w(F_o^2 - F_c^2)^2 / (N_{\text{obs}} - N_{\text{params}})]^{1/2}$$

Results and discussion

Syntheses of the complexes

The multi-dentate Schiff base ligand H₂L² was prepared by 1:2 condensation of diethylenetriamine and *o*-vaniline in methanol.⁸ The reaction of H₂L² with Ni(NO₃)₂·6H₂O in different stoichiometric ratios produces complexes 2–4 (Scheme 1). When ligand H₂L² was reacted with Ni(NO₃)₂·6H₂O in 1:1 molar ratio at room temperature in methanol solution, complex 2 was formed. It was a cocrystal of two mononuclear Ni^{II} units, [NiL¹]⁺ and [(Ni(HL²))]⁺. Addition of triethylamine (equimolar amount) to the solution did not make any difference in the composition of the resulted complex. The monocondensed ligand HL¹ was formed during the course of reaction *via* hydrolysis of dicondensed ligand H₂L². Previously,

the complexes of such ligands derived from the monocondensation of diethylenetriamine and an aromatic carbonyl compound with various metal ions were synthesized simply by 1:1 condensations of diethylenetriamine and *o*-vaniline in methanol and then reacting the ligand with corresponding metal salt in 1:1 molar ratio.¹⁵ We tried to prepare complex **1** following this method but the attempt was unsuccessful as the product was found to be complex **2**. Hence, for preparation of complex **1**, we developed here a new method, analogous to the monocondensation of 1,3-propanediamine with aromatic carbonyl compounds^{3b,6a,16} (detailed method is given in the experimental section).



Scheme 1. Syntheses of complexes 1–4.

In fact, the method was a Ni^{II} template synthesis where the tetra-coordinated square planar geometry of the resulting complex [NiL¹]⁺ was exploited. Complexes **3** and **4** were prepared by the reaction of H₂L² with Ni(NO₃)₂·6H₂O in 1:2 and 1:3 molar ratio, respectively in presence of triethylamine. In complex **4**, two *o*-vanillin molecules which were formed by the hydrolysis of H₂L² during complex formation, were also coordinated to the Ni^{II} centers along with Schiff base ligand H₂L². As a result, the yield was very low. However, when stoichiometric amount of *o*-vanillin was added to the reaction mixture, the yield of complex **4** was increased considerably (detailed method is given in the experimental section).

Description of the structures

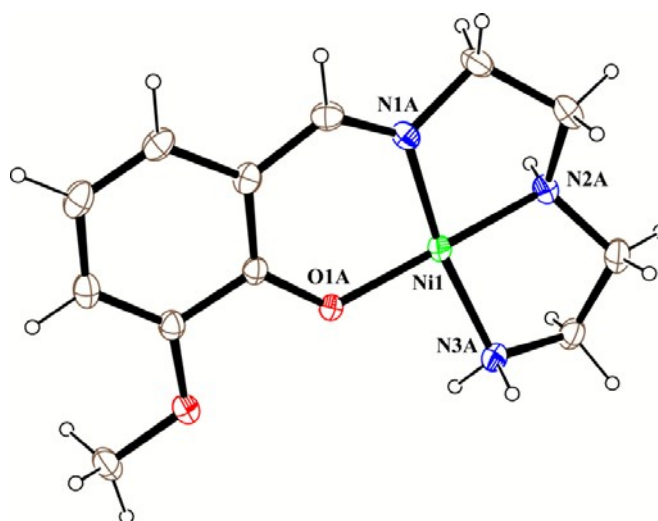


Fig. 1: ORTEP diagram of complex **1A** with 20% ellipsoid probability. Nitrate anions and solvent waters are not shown for clarity. The structure of **1B** is equivalent.

Complex 1

The asymmetric unit of complex **1** contains two independent cationic complex units (called A and B), two nitrate ions that balance the charge and three solvent water molecules. A perspective view of molecule A together with selective atomic numbering scheme is shown in Fig. 1. and that of B is presented in S1, ESI. Both units have equivalent structure with slight difference in bond angles and bond lengths. The Ni^{II} center possesses tetra-coordinated distorted square planar geometry being coordinated by two amine nitrogen atoms (N2A, N3A for Ni1 and N2B, N3B for Ni2), one imine nitrogen atom (N1A and N1B for Ni1 and Ni2, respectively) and one phenoxido oxygen atom (O1A for Ni1 and O2B for Ni2) of the Schiff

base ligand, HL¹. The Ni–N and Ni–O bond lengths are in the ranges of 1.829(4)–1.917(4) Å and 1.826(3)–1.830(4) Å, respectively. The selected bond lengths and angles are listed in Table S1, ESI. The r.m.s. (root mean squared) deviations of the four coordinated atoms in the basal planes are 0.115 and 0.096 Å around Ni1 and Ni2, respectively. The geometry around the Ni^{II} atom is confirmed by the (τ_4) index.¹⁷ The τ_4 values of Ni^{II} atoms are 0.126 and 0.113 for Ni1 and Ni2, respectively, indicating that the geometries are slightly distorted square planar for both Ni^{II} atoms. The mononuclear units are linked to each other through several hydrogen bonds (Table S5, ESI) to form a one-dimensional chain as shown in S2, ESI.

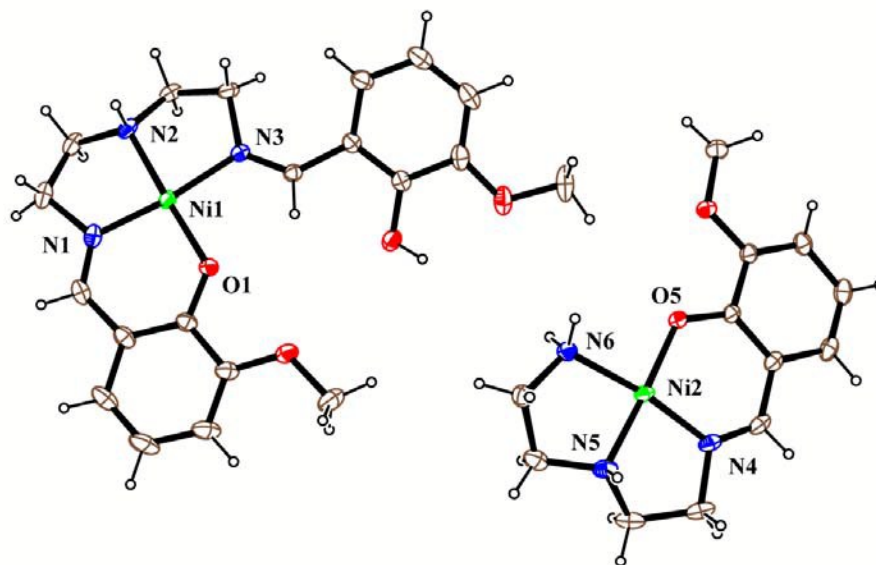


Fig. 2: ORTEP diagram of complex **2** with 20% ellipsoid probability. Nitrate anions and solvent water are not shown for clarity.

Complex 2

The asymmetric unit of complex **2** contains two independent mononuclear Ni^{II} units of two different Schiff base ligands HL¹ and H₂L², two nitrate ions and one water molecule. Both the Ni(II) centers have square planar geometry. The Ni1 center is coordinated by two imine nitrogen atoms (N1 and N3), one amine nitrogen atom (N2) and one phenoxido oxygen atom (O1) of singly deprotonated dicondensed Schiff base ligand (HL²)[−]. The Ni2 center is bonded by two amine nitrogen atoms (N5 and N6), one imine nitrogen atom (N4) and one phenoxido oxygen atom (O5) of monocondensed Schiff base ligand HL¹. Here, the Ni–N bond lengths are in the range 1.837(2)–1.922(2) Å. The Ni–O(phenoxido) bond lengths are 1.824(2) and

1.828(2) Å. The selected bond lengths and angles of both the complex units of **2** are listed in Table S2 (ESI). The r.m.s. deviations of the four coordinated atoms in the basal planes around the Ni1 and Ni2 centres are 0.037 and 0.038 Å, respectively. Here the τ_4 values of Ni^{II} atoms are 0.079 and 0.075 for Ni1 and Ni2, respectively, indicating that the geometries are nearly square planar. The two mononuclear units form a three dimensional network as shown in Fig. S3 (ESI) *via* several intermolecular hydrogen bonding interactions (Table S5, ESI).

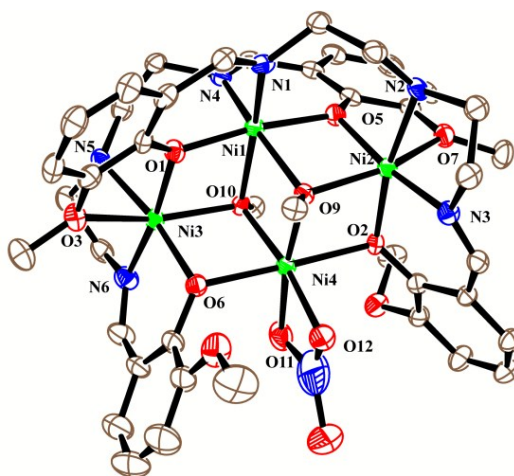


Fig. 3: ORTEP diagram of complex **3** with 20% ellipsoid probability. Hydrogen atoms, nitrate anion and solvent methanol are not shown for clarity.

Complex 3

Complex **3** has a tetranuclear structure with a defective cubane core where four Ni^{II} centers are bridged *via* two μ_3 -methoxido ions. The asymmetric unit of this complex consists of two deprotonated Schiff base ligands (L²)²⁻, two methoxido ions and one chelating nitrate co-anion along with four Ni^{II} ions. One non-coordinating nitrate ion and a solvent methanol molecule remain outside of the coordination sphere. The structure of complex **3** is shown in Fig. 3 together with selective atomic numbering scheme. Here, all the Ni^{II} ions have a hexacoordinated distorted octahedral geometry. The Ni1 centre is bonded by the four donor atoms of the two Schiff base ligands (O1, N1 and O5, N4) and two μ_3 -bridged oxygen atoms of methoxido ions (O9 and O10). Each of the Ni2 and Ni3 centers are coordinated by three donor atoms of one Schiff base ligand (O2, N2, N3 for Ni2 and O6, N5, N6 for Ni3) and two oxygen atoms of another Schiff base ligand (O5, O7 for Ni2, and O1, O3 for Ni3) and one μ_3 -bridged oxygen atom of methoxido ion (O9 for Ni2 and O10 for Ni3). The Ni4 center is coordinated by two phenoxido oxygen atoms (O2 and O6) of two Schiff base ligands, two μ_3 -

methoxido oxygen atoms (O9 and O10) and the two oxygen atoms (O11 and O12) of the chelating nitrate ion. The Ni–N and Ni–O bond lengths are within the ranges of 1.972(9)–2.142(9) Å and 1.925(7)–2.134(6) Å, respectively. The selected bond lengths and angles of complex **3** are listed in Table S3, ESI. The complex shows several intermolecular hydrogen bonding interactions (Fig. S4, ESI).

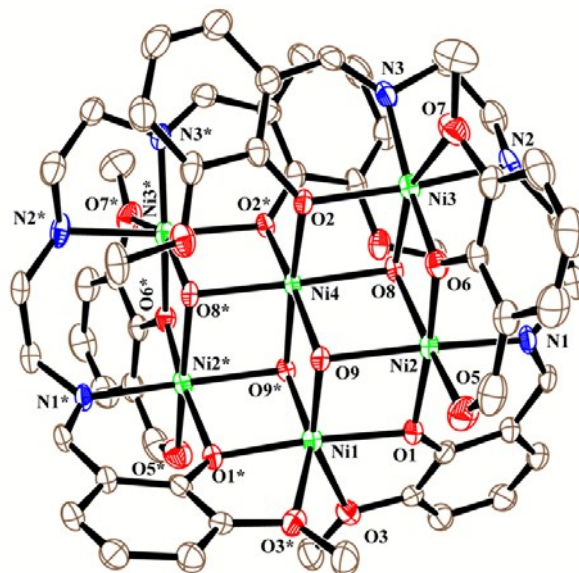


Fig. 4: ORTEP diagram of complex **4** with 20% ellipsoid probability. Hydrogen atoms, nitrate anions and solvent water are not shown for clarity.

Complex 4

Complex **4** possesses a discrete hexa-nuclear Ni₆ structure with two fused defective cubane cores, having a crystallographic C₂ axis passing through the Ni1, Ni4 centers. All six Ni^{II} centers are hexa-coordinated with distorted octahedral geometry. The asymmetric unit contains four Ni^{II} ions, one deprotonated Schiff base ligand (L²)²⁻, one deprotonated *o*-vaniline co-ligand (*o*-van) and one nitrate ion. A non-coordinating water molecule remains outside the coordination core. The structure of complex **4** is shown Fig. 4 together with selective atomic numbering scheme. The Ni1 center is coordinated by two symmetry related phenoxido oxygen (O1, O1*), two methoxido oxygen (O3, O3*) of two ligand H₂L² and two μ_3 -bridged hydroxido oxygen atoms (O9, O9*) where symmetry element * = 1-x,y,3/2-z. Similarly, Ni4 center is coordinated by two symmetry related phenoxido oxygen (O2, O2*) and four μ_3 -bridged hydroxido oxygen atoms (O8, O8* and O9, O9*). The Ni2 center is

coordinated by one nitrogen atom and five oxygen atoms; N1 and O1 from H₂L², O5 and O6 from *o*-vaniline, O9 and O8 of two μ_3 -bridged hydroxido ions. On the other hand, Ni³ center is coordinated by two nitrogen atoms and four oxygen atoms; N2, N3 and O2 from H₂L², O6 and O7 from *o*-vaniline, and O8 from μ_3 -bridged hydroxido ion. The Ni–N and Ni–O bond lengths are in the range of 1.959(9)–2.120(1) Å, and 1.954(7)–2.126(5) Å, respectively. The selected bond lengths and angles of complex **4** are listed in Table S4, ESI. The hydrogen bonding interactions present in complex **4** is shown in Fig. S5 (ESI). Details of the hydrogen bonding interactions are given in Table S5, ESI.

A CSD search reveals that the ligand, *N,N'*-bis(3-methoxysalicylidene)diethylenetriamine) (H₂L²) has been used mostly for the synthesis of lanthanide complexes. The homo-metallic Ln-complexes are usually dinuclear^{7a,7g} but one mono-^{7h} and two dodeca-nuclear⁷ⁱ complexes are also known where as the heterometallic complexes containing Ln^{III} are found to be tri-, hexa- and poly-nuclear.^{7b,7c,7d,7f} In contrast, this ligand has rarely been used for the synthesis of transition metal complexes and till date, only one each of dinuclear Mn^{II}, di- and tetranuclear Cu^{II} complexes are reported.^{7e,7j} In addition, three dinuclear Zn^{II} and two trinuclear Cd^{II} complexes are also known.¹⁸ Recently, we used this ligand for the synthesis of Zn^{II} complexes and obtained a di-, a tetra- and a hexa-nuclear complexes.⁸ Thus complexes **2**, **3** and **4** of present paper are the first report of Ni^{II} complexes of this ligand. On the other hand, only one Ni^{II} and one Cu^{II} complexes of the mono-condensed ligand, HL¹ is reported till date and both of these complexes are mononuclear.^{15,19}

Magnetic Properties

Among the four complexes, Ni^{II} centres are diamagnetic with square planar geometry in complexes **1** and **2**. Therefore, the temperature dependent molar magnetic susceptibility measurements were performed only for complexes **3** and **4**. Thermal variations of the product of molar magnetic susceptibility with temperature ($\chi_M T$) for complexes **3** and **4** are shown in Fig. 5. The room temperature $\chi_M T$ value for complex **3** is 5.40 cm³ K mol⁻¹, which is higher than the value of magnetically noninteracting Ni^{II}₄ system of 4.0 cm³ K mol⁻¹ for $g_{Ni} = 2.1$ at 300 K; whereas for complex **4**, the $\chi_M T$ value is 5.55 cm³ K mol⁻¹, which is slightly lower than the value of magnetically noninteracting Ni^{II}₆ system of 6.0 cm³ K mol⁻¹ for $g_{Ni} = 2.1$ at 300 K.²¹ The temperature dependence of $\chi_M T$ is different for complexes **3** and **4**. In case of

complex **3**, the χ_{MT} value gradually increases upon cooling down to 50 K and below this temperature, it sharply increases and reaches the maximum of $8.82 \text{ cm}^3 \text{ K mol}^{-1}$ at 6 K. On further cooling, the χ_{MT} value starts to decrease and reaches to $7.89 \text{ cm}^3 \text{ K mol}^{-1}$ at 2 K. This increasing nature of χ_{MT} value on lowering the temperature, indicates overall intramolecular ferromagnetic coupling between the metal ions in complex **3**. For complex **4**, the χ_{MT} value gradually decreases upon cooling to 60 K and below this temperature it sharply decreases and reaches to $1.25 \text{ cm}^3 \text{ K mol}^{-1}$ at 2.5 K. Here, the decreasing nature of χ_{MT} value with decreasing temperature indicates the intramolecular antiferromagnetic interaction between the metal ions. The field dependent molar magnetizations values ($M/N\beta$) up to 5 T magnetic fields are $6.91 \mu_B$ for complex **3** at 2 K and $2.62 \mu_B$ for complex **4** at 2.5 K (Fig. S6, ESI). The magnetization values of both complexes increase with increasing the field but the nature of enhancement indicates that the magnetic coupling in **3** is ferromagnetic where as that in **4** is antiferromagnetic.^{20,21}

The structure of tetranuclear complex **3** is defective cubane, where Ni^{II} centres are connected *via* both phenoxido and μ_3 -methoxido oxygen atoms (Fig. 6, left). In this complex, two different types of bridging are observed between the Ni^{II} centres: i) bridging *via* one phenoxido and one μ_3 -methoxido oxygen atoms and ii) bridging *via* two μ_3 -methoxido oxygen atoms. Therefore, for simulation of the magnetic data of complex **3**, we have considered two exchange couplings; J_1 for both phenoxido and μ_3 -methoxido bridged Ni^{II} ($S = 1$) centres and J_2 for double μ_3 -methoxido bridged Ni^{II} ($S = 1$) centres. The Hamiltonian used for the simulation of χ_{MT} data of complex **3** is written as $H = -J_1(S_1S_2 + S_1S_3 + S_2S_4 + S_3S_4) - J_2(S_2S_3)$, where $S_1 = S_2 = S_3 = S_4 = S_{\text{Ni}}$. The interaction between two Ni^{II} centres, S_1 and S_4 are taken as zero due to the long intranuclear $\text{Ni}^{\text{II}} \dots \text{Ni}^{\text{II}}$ distance. Complex **4** has a hexanuclear Ni^{II}_6 structure, where two defective cubane like cores are symmetrically fused together perpendicularly (Fig. 6, right). In this complex, Ni^{II} centres are connected *via* both phenoxido and μ_3 -hydroxido oxygen atoms and a crystallographic C_2 axis is passing through the two Ni^{II} atoms by which two defective cubanes are fused to each other. Here also, two different types of bridging are observed between the Ni^{II} centres: i) bridging *via* one phenoxido and one μ_3 -hydroxido oxygen atoms, and ii) bridging *via* two μ_3 -hydroxido oxygen atoms. For simulation of the magnetic data of complex **4** we have considered four exchange couplings depending on the bridging angles between Ni^{II} centres; J_1 and J_2 for both phenoxido and μ_3 -hydroxido bridged Ni^{II} ($S = 1$) centres, and J_3 and J_4 for double μ_3 -

hydroxido bridged Ni^{II} ($S = 1$) centres. The Hamiltonian used for the simulation of χ_{MT} data of complex **4** is written as $H = -J_1(S_1S_2 + S_5S_6) - J_2(S_1S_3 + S_2S_4 + S_3S_6 + S_4S_5) - J_3(S_2S_3 + S_3S_5) - J_4(S_3S_4)$, where $S_1 = S_2 = S_3 = S_4 = S_5 = S_6 = S_{Ni}$. The other exchange interactions between Ni^{II} centres, S_1-S_4 , S_1-S_6 and S_4-S_6 are taken as zero due to the long intranuclear Ni^{II}.....Ni^{II} distances. The simulations of experimental χ_{MT} data of both complexes **3** and **4** were carried out using the PHI program taking into account the molecular field approximations.²² The best fittings were obtained using the following set of parameters: $J_1 = 0.64 \text{ cm}^{-1}$, $J_2 = 8.41 \text{ cm}^{-1}$, $g_{Ni} = 2.28$, $R = 6.56 \times 10^{-4}$ for complex **3**; $J_1 = -5.60 \text{ cm}^{-1}$, $J_2 = -9.39 \text{ cm}^{-1}$, $J_3 = -5.18 \text{ cm}^{-1}$, $J_4 = 3.72 \text{ cm}^{-1}$, $R = 1.41 \times 10^{-4}$ for complex **4**, where $R = \frac{\sum[(\chi_{MT})_{exp.} - (\chi_{MT})_{calcd.}]^2}{\sum((\chi_{MT})_{exp})^2}$. The g value of Ni is fixed at $g_{Ni} = 2.20$ for complex **4** during simulation.

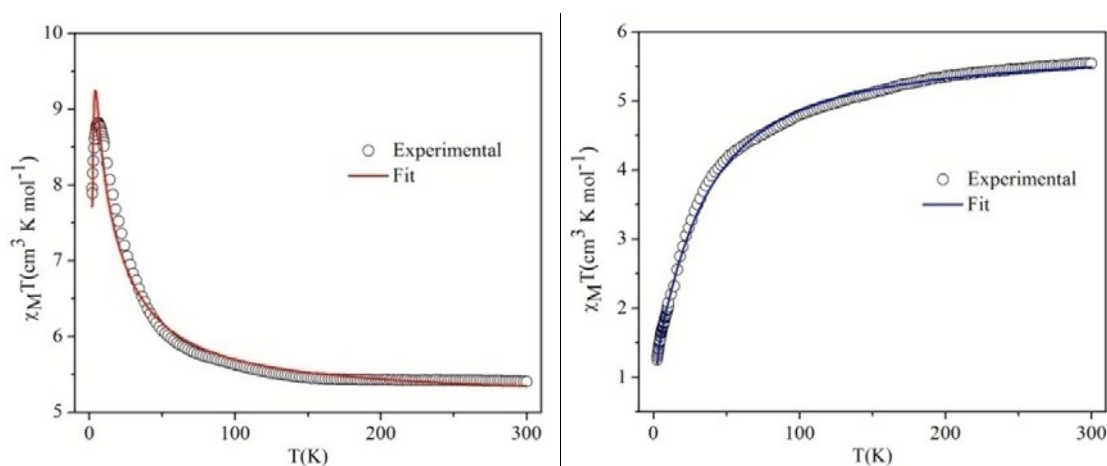


Figure 5: Thermal variations of the χ_{MT} products for complexes **3** and **4** (left to right respectively). Solid red line represents the best fitting to the appropriate model for **3** and solid blue line represents the best fitting to the appropriate model for **4**.

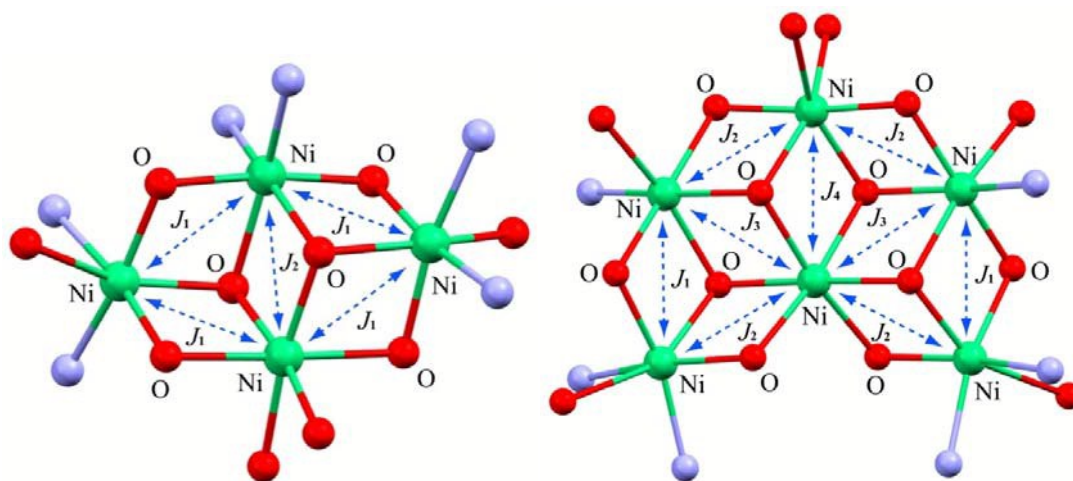


Figure 6: Basic tetranuclear core of complex **3** (left) and hexanuclear core of complex **4** (right) with different magnetic exchange couplings (J).

Magneto-structural correlations

A lot of di-phenoxido, di-alkoxido and di-hydroxido bridged Ni^{II} complexes which have been characterized both structurally and magnetically are reported and their magneto-structural correlations are well-established.²³ The factors affecting the exchange interaction in these complexes are: Ni–O–Ni bridging angle (θ), deviation of phenyl/alkyl carbon from the Ni₂O plane (τ), Ni...Ni distances and the hinge angle between two O–Ni–O planes (β). Among these, the most important factor is the Ni–O–Ni bridging angle (θ) as the sign and magnitude of exchange coupling is very much dependant on this angle.²⁴ From the reported magneto-structural correlations, it is found that the ferro- to antiferromagnetic crossover angle for such complexes is ~ 96 – 98° . Although it is also found that the antiferromagnetic coupling increases with decrease in τ and β angles, a nearly linear relationship is observed between exchange coupling and average Ni–O–Ni angle for such complexes, where antiferromagnetic coupling increases with increase in Ni–O–Ni angle.²⁴

Complex **3** shows two types of exchange pathways; coupling constants J_1 and J_2 are assigned to μ -phenoxido/ μ_3 -methoxido bridge and double μ_3 -methoxido bridge, respectively. The four average μ -phenoxido/ μ_3 -methoxido bridging angles (97.97° , 98.38° , 98.34° and 98.57°) are very close, therefore same exchange coupling (J_1) is considered for these angles. The average Ni–O–Ni bridging angles for J_1 and J_2 are 98.3° and 97.57° respectively. Complex **4**

possesses a C_2 symmetry and here for the two μ -phenoxido/ μ_3 -hydroxido bridges two different exchange coupling constants, J_1 and J_2 are considered as the average Ni–O–Ni bridging angles (98.13° and 99.56°) for the two bridges are different. Similarly for the double μ_3 -hydroxido bridges, two different coupling constant J_3 and J_4 are considered as the average Ni–O–Ni bridging angles are 98.62° and 96.79° , respectively. Fig. 7 (left) shows an approximate linear dependence of exchange coupling (J) with corresponding mixed μ -phenoxido/ μ_3 -OR (R = Me/H) bridged Ni–O–Ni angles in some previously reported defective cubane like Ni^{II} complexes (Table S6, ESI), where antiferromagnetic coupling increases with increase in average Ni–O–Ni angle. From this plot as shown in Fig. 7 (left), it is apparent that the crossover angle is $\sim 97^\circ$ for this type of bridging. The sign and magnitude of exchange couplings; J_1 in **3** and J_1 and J_2 in **4** show good agreement with their corresponding average Ni–O–Ni bridging angles in this correlation. Fig. 7 (right) shows similar linear dependence of exchange coupling with corresponding double μ_3 -OR (R = Me/H) bridged Ni–O–Ni angles in some earlier reported defective cubane or cubane like Ni^{II} complexes (Table S6, ESI). The sign and magnitude of exchange couplings; J_2 in **3** and J_3 and J_4 in **4** agree well with the general trend of linear dependence with their corresponding average Ni–O–Ni bridging angles. In case of μ_3 -OR (R = Me/H) bridged cubane like Ni^{II} complexes, it is noticed that the crossover angle is $\sim 99^\circ$ for such type of bridging.²⁵ However, one should be cautious on mentioning the exact crossover angle as other factors like τ and β can affect the exchange interactions and the points are highly scattered.

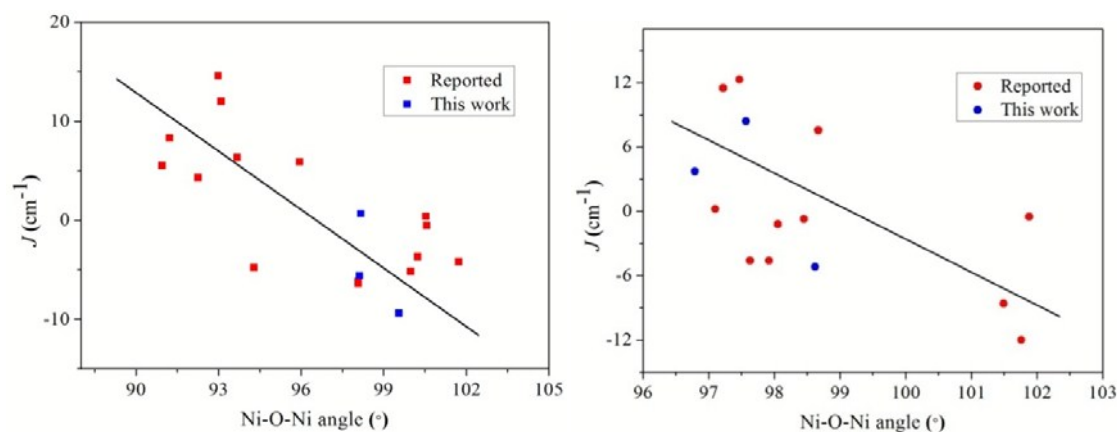


Figure 7: Variation of the magnetic exchange coupling (J) in cubane and defective cubane like Ni^{II} complexes with mixed μ -phenoxido/ μ_3 -OR (R = Me/H) bridged (left) and double μ_3 -OR (R = Me/H) bridged average Ni–O–Ni angles (right).

Electrochemistry

Cyclic voltammograms (CVs) of all complexes **1–4** were recorded in acetonitrile with respect to an Ag/AgCl electrode at a scan rate of 100 mV/sec. On forward cathodic scan (0 to -1.8 V) only one wave appeared in the cyclic voltammograms of complexes **1**, **3** and **4** (Fig. 8) for the reduction process at the electrode surface. The peaks were observed at $E_c = -1.43$ V for complex **1**, $E_c = -1.65$ V for complex **3** and $E_c = -1.48$ V for complex **4**. The appearance of one peak on forward scan in each of these complexes suggests the single step reduction of Ni^{II} to Ni^{I} in these complexes. In case of cyclic voltammogram of complex **2**, two waves appeared on forward cathodic scan. Here, the two peaks were observed at $E_c = -1.44$, and $E_c = -1.55$ V. The potential difference ($\Delta E_{12} = E_1 - E_2$)²⁶ between two consecutive peaks was -0.11 V for complex **2**. The appearance of two peaks in the cyclic voltammogram of complex **2** indicates the presence of two different Ni(II) species in the solution. Complex **2** contains two Ni^{II} species i.e. $\text{Ni}(\text{L}^1)^+$ and $\text{Ni}(\text{HL}^2)^+$ of two different ligands.²⁷ Therefore, during reduction of Ni^{II} to Ni^{I} two consecutive peaks are observed in the cyclic voltammogram of complex **2**. On reverse scan, cyclic voltammograms of all complexes **1–4** do not show any prominent peak for the oxidation of Ni^{I} to Ni^{II} , which implies that the reduction processes of Ni^{II} species are irreversible for each of the complexes.

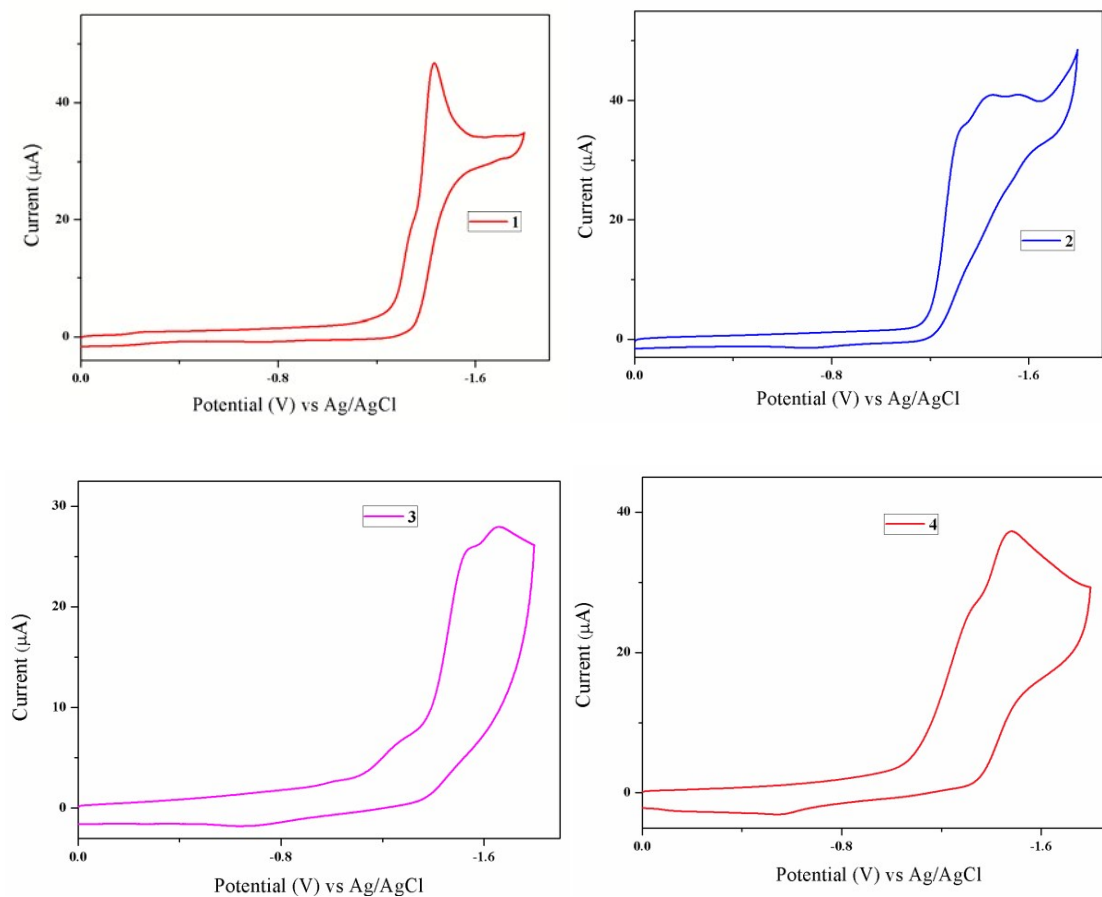


Figure 8: Cyclic voltammograms of complexes **1–4** which are recorded in acetonitrile (0.1 M TBAP) with a glassy carbon working electrode at the scan rate of 100 mVs⁻¹.

Conclusions

We have reacted the flexidentate ligand, *N,N*-bis(3-methoxysalicylidene)diethylenetriamine) (H_2L^2) having seven potential donor atoms with nickel nitrate by changing the metal:ligand ratios and obtained one each of mono-, tetra- and hexanuclear complexes. These are the first report of the synthesis of Ni^{II} complexes with the ligand H_2L^2 . The mononuclear complex $[NiHL^2]$ was isolated as cocrystal along with another complex $[NiL^1]$. HL^1 is the monocondensed product of diethylenetriamine and *o*-vaniline. It was formed by the hydrolysis of H_2L^2 during the synthesis. To obtain pure $[NiL^1]$, we successfully developed a new template method, exploiting the square planar geometry of Ni^{II}. In this report, by isolating mono-, tetra- and hexa-nuclear complexes, we have also shown that the nuclearity

of the resulting Ni^{II} complexes of the ligand (H₂L²) can be controlled simply by monitoring the proportion of the reactants and the reaction conditions. The magnetic characterization reveals that the Ni^{II} ions were ferromagnetically coupled in complex **3** whereas the coupling was antiferromagnetic in complex **4**. Thus, these two complexes are unique examples showing the reversal of magnetic coupling on changing the nuclearity of the complex and bridging ligand from μ_3 -methoxido to μ_3 -hydroxido. Careful inspection of the structural parameters revealed that these changes brought about slight difference in the bridging angles. As the bridging angles in these complexes are close to the crossover angle, these changes, albeit very small, are good enough for this reversal of magnetic coupling.

Acknowledgements

T. K. G. is thankful to the University Grants Commission (UGC), New Delhi, for Senior Research Fellowship [Sr. no. 2061510191, Ref. no. 21/06/2015 (I) EU-V, dated 15/12/2015]. P. M. is thankful to the Council of Scientific and Industrial Research (CSIR), Government of India for the Senior Research Fellowship [Sanction no. 09/02(0935)/2014-EMR-I]. A. G. thanks CRNN, University of Calcutta, Kolkata, India for the magnetic measurement. We thank USIC, The University of Burdwan, West Bengal, India, for providing the single-crystal X-ray diffractometer facility.

Supporting Information (see footnote on the first page of this article): ORTEP diagram of complex **1B**, Description of IR spectra, pictures of hydrogen bonding interactions, table of bond length and bond angles parameters and hydrogen bonding parameters of complexes **1–4** as well as magnetization plots of complexes **3–4**. CCDC 1907763 (for **1**), 1907764 (for **2**), 1907765 (for **3**) and 1907766 (for **4**) contain the supplementary crystallographic data for this paper. These data can be obtained free of charge from The Cambridge Crystallographic Data Centre via www.ccdc.cam.ac.uk/data_request/cif.

References

- 1 (a) S. W. Ragsdale, *Journal of Biological Chem.*, 2009, **284**, 18571–18575; (b) M. A. Halcrow and G. Christou, *Chem. Rev.*, 1994, **94**, 2421–2481.
- 2 (a) G. A. Craig and M. Murrie, *Chem. Soc. Rev.*, 2015, **44**, 2135–2147; (b) G. E. Kostakis, A. M. Ako and A. K. Powell, *Chem. Soc. Rev.*, 2010, **39**, 2238–2271; (c) S. Ghosh, S. Mukherjee, P. Seth, P. S. Mukherjee and A. Ghosh, *Dalton Trans.*, 2013, **42**, 13554–13564; (d) M. Andruh, *Chem. Commun.*, 2018, **54**, 3559–3577; (e) A. Hazaria, T. K. Ghosh, C. J. Gómez-García and A. Ghosh, *Inorg. Chim. Acta*, 2018, **471**, 168–175.
- 3 (a) D. Krishnamurthy, A. N. Sarjeant, D. P. Goldberg, A. Caneschi, F. Totti, L. N. Zakharov and A. L. Rheingold, *Chem. Eur. J.*, 2005, **11**, 7328–7341; (b) P. Mahapatra, S. Giri, M. G. B. Drew and A. Ghosh, *Dalton Trans.*, 2018, **47**, 3568–3579; (c) L.-S. Long, *CrystEngComm.*, 2010, **12**, 1354–1365; (d) A. Das, S. Jana and A. Ghosh, *Cryst. Growth Des.*, 2018, **18**, 2335–2348.
- 4 (a) P. Chakraborty, J. Adhikary, B. Ghosh, R. Sanyal, S. K. Chattopadhyay, A. Bauzá, A. Frontera, E. Zangrando and D. Das, *Inorg. Chem.*, 2014, **53**, 8257–8269; (b) A. Biswas, L. K. Das, M. G. B. Drew, G. Aromí, P. Gamez and A. Ghosh, *Inorg. Chem.*, 2012, **51**, 7993–8001; (c) T. Chakraborty, S. Mukherjee, S. Dasgupta, B. Biswas and D. Das, *Dalton Trans.*, 2019, **48**, 2772–2784.
- 5 (a) A. Bell, G. Aromí, S. J. Teat, W. Wernsdorfer and R. E. P. Winpenny, *Chem. Commun.*, **2005**, 2808–2810; (b) S. Petit, P. Neugebauer, G. Pilet, G. Chastanet, A.-L. Barra, A. B. Antunes, W. Wernsdorfer and D. Luneau, *Inorg. Chem.*, 2012, **51**, 6645–6654; (c) B. X.-T. Liu, X.-Y. Wang, W.-X. Zhang, P. Cui and S. Gao, *Adv. Mater.*, 2006, **18**, 2852–2856; (d) M. Moragues-Cánovas, M. Helliwell, L. Ricard, È. Rivière, W. Wernsdorfer, E. Brechin and T. Mallah, *Eur. J. Inorg. Chem.*, 2004, 2219–2222; (e) C. Cadiou, M. Murrie, C. Paulsen, V. Villar, W. Wernsdorfer and R. E. P. Winpenny, *Chem. Commun.*, 2001, 2666–2667; (f) S. Hameury, L. Kayser, R. Pattacini, P. Rosa, A.-L. Barra and P. Braunstein, *ChemPlusChem*, 2015, **80**, 1312–1320.
- 6 (a) P. Mahapatra, M. G. B. Drew and A. Ghosh, *Inorg. Chem.*, 2018, **57**, 8338–8353; (b) S. Biswas, S. Naiya, C. J. Gómez-García and A. Ghosh, *Dalton Trans.*, 2012, **41**, 462–473.

7 (a) F. Habib, G. Brunet, V. Vieru, I. Korobkov, L. F. Chibotaru and M. Murugesu, *J. Am. Chem. Soc.*, 2013, **135**, 13242–13245; (b) C.-M. Liu, D.-Q. Zhang, X. Hao and D.-B. Zhu, *Chem. Asian J.*, 2014, **9**, 1847–1853; (c) G. Brunet, F. Habib, I. Korobkov and M. Murugesu, *Inorg. Chem.*, 2015, **54**, 6195–6202; (d) L. Zhao, J. Wu, H. Ke and J. Tang, *Inorg. Chem.*, 2014, **53**, 3519–3525; (e) L.-F. Zou, L. Zhao, Y.-N. Guo, J. Tang, Q.-L. Wang and Y.-H. Li, *Inorg. Chim. Acta*, 2012, **382**, 65–71; (f) X.-C. Huang, M. Zhang, D. Wu, D. Shao, X.-H. Zhao, W. Huang and X.-Y. Wang, *Dalton Trans.*, 2015, **44**, 20834–20838; (g) J. Long, F. Habib, P.-H. Lin, I. Korobkov, G. Enright, L. Ungur, W. Wernsdorfer, L. F. Chibotaru and M. Murugesu, *J. Am. Chem. Soc.*, 2011, **133**, 5319–5328; (h) W. Dou, J.-N. Yao, W.-S. Liu, Y.-W. Wang, J.-R. Zheng and D.-Q. Wang, *Inorg. Chem. Commun.*, 2007, **10**, 105–108; (i) L. Zhao, S. Xue and J. Tang, *Inorg. Chem.*, 2012, **51**, 5994–5996; (j) K. Das, C. Patra, C. Sen, A. Datta, C. Massera, E. Garribba, M. S. E. Fallah, B. B. Beyene, C.-H. Hung, C. Sinha, T. Askun, P. Celikboyun, D. Escudero and A. Frontera, *J. Biol. Inorg. Chem.*, 2017, **22**, 481–495.

8 T. K. Ghosh, S. Jana and A. Ghosh, *Inorg. Chem.*, 2018, **57**, 15216–15228.

9 (a) R. Biswas, Y. Ida, M. L. Baker, S. Biswas, P. Kar, H. Nojiri, T. Ishida and A. Ghosh, *Chem. Eur. J.*, 2013, **19**, 394–3953; (b) L. K. Das, A. Biswas, J. S. Kinyon, N. S. Dalal, H. Zhou and A. Ghosh, *Inorg. Chem.*, 2013, **52**, 11744–11757; (c) A. K. Ghosh, M. Shatruck, V. Bertolasi, K. Pramanik and D. Ray, *Inorg. Chem.*, 2013, **52**, 13894–13903; (d) C. Papatriantafyllopoulou, G. Aromi, A. J. Tasiopoulos, V. Nastopoulos, C. P. Raptopoulou, S. J. Teat, A. Escuer and S. P. Perlepes, *Eur. J. Inorg. Chem.*, 2007, 2761–2774; (e) S. T. Meally, C. McDonald, G. Karotsis, G. S. Papaefstathiou, E. K. Brechin, P. W. Dunne, P. McArdle, N. P. Power and L. F. Jones, *Dalton Trans.*, 2010, **39**, 4809–4816; (f) E. K. Brechin, W. Clegg, M. Murrie, S. Parsons, S. J. Teat and R. E. P. Winpenny, *J. Am. Chem. Soc.*, 1998, **120**, 7365–7366; (g) Y. N. Shvachko, D. V. Starichenko, A. V. Korolev, A. V. Pestov, P. A. Slepukhin and D. W. Boukhvalov, *Inorg. Chim. Acta*, 2018, **483**, 480–487; (h) S. T. Ochsenein, M. Murrie, E. Rusanov, H. Stoeckli-Evans, C. Sekine and H. U. Guldell, *Inorg. Chem.*, 2002, **41**, 5133–5140; (i) A. Bilyk, J. W. Dunlop, R. O. Fuller, A. K. Hall, J. M. Harrowfield, M. W. Hosseini, G. A. Koutsantonis, I. W. Murray, B. W. Skelton, R. L. Stamps and A. H. White, *Eur. J. Inorg. Chem.*, 2010, 2106–2126.

- 10 P. Mukherjee, M. G. B. Drew and A. Ghosh, *Eur. J. Inorg. Chem.*, 2008, 3372–3381.
- 11 A. K. Mukherjee, S. Koner, A. Ghosh, N. R. Chaudhuri, M. Mukherjee and A. J. Welch, *J. Chem. Soc., Dalton Trans.*, 1994, **0**, 2367–2371.
- 12 G. M. Sheldrick, SHELX. *Acta Crystallogr., Sect. A: Found. Crystallogr.* 2008, **64**, 112–122.
- 13 O. V. Dolomanov, L. J. Bourhis, R. J. Gildea, J. A. K Howard and H. Puschmann, *J. Appl. Crystallogr.*, 2009, **42**, 339–341.
- 14 SAINT and SADABS, version 6.02 and version 2.03, Bruker AXS, Inc., Madison, WI, 2002.
- 15 A. Bhunia, S. Manna, S. Mistri, A. Paul, R. K. Manne, M. K. Santra, V. Bertolasi and S. C. Manna, *RSC Adv.*, 2015, **5**, 67727–67737.
- 16 P. Mahapatra, A. Bauzá, A. Frontera, M. G. B. Drew and A. Ghosh, *Inorg. Chim. Acta*, 2018, **477**, 89–101.
- 17 L. Yang, D. R. Powell and R. P. Houser, *Dalton Trans.*, 2007, 955–964.
- 18 (a) B. Naskar, R. Modak, D. K. Maiti, M. G. B. Drew, A. Bauzá, A. Frontera, C. D. Mukhopadhyay, S. Mishra, K. D. Saha and S. Goswami, *Dalton Trans.*, 2017, **46**, 9498–9510; (b) J. Chakraborty, S. Thakurta, B. Samanta, A. Ray, G. Pilet, S. R. Batten, P. Jensen and S. Mitra, *Polyhedron*, 2007, **26**, 5139–5149.
- 19 (a) K. Das, G. W. Woyessa, A. Datta, B. B. Beyene, S. Goswami, E. Garribba, A. Frontera and C. Sinha, *J. Mol. Str.*, 2018, **1173**, 462–468.
- 20 (a) T. Nakajima, K. Seto, A. Scheurer, B. Kure, T. Kajiwara, T. Tanase, M. Mikuriya and H. Sakiyama, *Eur. J. Inorg. Chem.*, 2014, 5021–5033; (b) I. Nemeč, R. Herchel, M. Machata and Z. Trávníček, *New J. Chem.*, 2017, **41**, 11258–11267; (c) D. Mandal, V. Bertolasi, J. Ribas-Ariño, G. Aromí and D. Ray, *Inorg. Chem.*, 2008, **47**, 3465–3467; (d) S. S. Tandon, S. D. Bunge, J. Sanchiz and L. K. Thompson, *Inorg. Chem.*, 2012, **51**, 3270–3282; (e) H.-Y. Zhang, Y. Li, W. Wang, X. Zhang, J.-M. Wang and S.-H. Zhang, *J. Coord. Chem.*, 2016, **69**, 1938–1948.

- 21 (a) R. Herchel, I. Nemeč, M. Machata and Z. Trávníček, *Dalton Trans.*, 2016, **45**, 18622–18634; (b) S. S. Tandon, S. D. Bunge, R. Rakosi, Z. Xu and L. K. Thompson, *Dalton Trans.*, 2009, 6536–6551; (c) S. Liu, S. Wang, F. Cao, H. Fu, D. Li and J. Dou, *RSC Adv.*, 2012, **2**, 1310–1313; (d) P. Mukherjee, M. G. B. Drew, C. J. Gómez-García and A. Ghosh, *Inorg. Chem.*, 2009, **48**, 5848–5860.
- 22 N. F. Chilton, R. P. Anderson, L. D. Turner, A. Soncini and K. S. Murray, *J. Comput. Chem.*, 2013, **34**, 1164–1175.
- 23 (a) L. Botana, J. Ruiz, A. J. Mota, A. Rodríguez-Diéguez, J. M. Seco, I. Oyarzabala and E. Colacio, *Dalton Trans.*, 2014, **43**, 13509–13524; (b) M. Das, R. Herchel, Z. Trávníček, V. Bertolasi and D. Ray, *New J. Chem.*, 2018, **42**, 16717–16728; (c) M. A. Halcrow, J.-S. Sun, J. C. Huffman and G. Christou, *Inorg. Chem.*, 1995, **34**, 4167–4177; (d) R. Biswas, S. Giri, S. K. Saha and A. Ghosh, *Eur. J. Inorg. Chem.*, **2012**, 2916–1927; (e) J. M. Clemente-Juan, B. Chansou, B. Donnadieu and J. P. Tuchages, *Inorg. Chem.*, 2000, **39**, 5515–5519; (f) M. Mondal, S. Giri, P. M. Guha and A. Ghosh, *Dalton Trans.*, 2017, **46**, 697–708.
- 24 (a) M. P. Palacios, A. J. Mota, J. E. Perea-Buceta, F. J. White, E. K. Brechin and E. Colacio, *Inorg. Chem.*, 2010, **49**, 10156–10165; (b) I. Oyarzabal, J. Ruiz, A. J. Mota, A. Rodríguez-Diéguez, J. M. Seco and E. Colacio, *Dalton Trans.*, 2015, **44**, 6825–6838.
- 25 (a) A. Das, F. J. Klinke, S. Demeshko, S. Meyer, S. Dechert and F. Meyer, *Inorg. Chem.*, 2012, **51**, 8141–8149; (b) M. A. Halcrow, J. S. Sun, J. C. Huffman and G. Christou, *Inorg. Chem.*, 1995, **34**, 4167–4177; (c) J. M. Clemente-Juan, B. Chansou, B. Donnadieu and J. P. Tuchages, *Inorg. Chem.*, 2000, **39**, 5515–5519.
- 26 (a) J. Ferrando-Soria, O. Fabelo, M. Castellano, J. Cano, S. Fordham and H. C. Zhou, *Chem. Commun.*, 2015, **51**, 13381–13384; (b) Y. Y. Zhou, D. R. Hartline, T. J. Steiman, P. E. Fanwick and C. Uyeda, *Inorg. Chem.*, 2014, **53**, 11770–11777.
- 27 (a) P. Mahapatra, S. Ghosh, S. Giri and A. Ghosh, *Polyhedron*, 2016, **117**, 427–436; (b) S. Anbu, M. Kandaswamy and B. Varghese, *Dalton Trans.*, 2010, **39**, 3823–3832; (c) P. Mahapatra, M. G. B. Drew and A. Ghosh, *Dalton Trans.*, 2018, **47**, 13957–13971.